International Journal of Radiation Oncology biology • physics

www.redjournal.org

Clinical Investigation

^{18}F-Fluorodeoxyglucose/Positron Emission Tomography Predicts Patterns of Failure After Definitive Chemoradiation Therapy for Locally Advanced Non-Small Cell Lung Cancer

Nitin Ohri, MD, MS,* William R. Bodner, MD,* Balazs Halmos, MD,† Haiying Cheng, MD, PhD,† Roman Perez-Soler, MD,† Steven M. Keller, MD,‡ Shalom Kalnicki, MD,* and Madhur Garg, MD*

*Departments of *Radiation Oncology, †Oncology, and ‡Cardiothoracic Surgery, Montefiore Medical Center, Albert Einstein College of Medicine, Bronx, New York*

Received Sep 22, 2016, and in revised form Oct 18, 2016. Accepted for publication Oct 19, 2016.

Summary

A previous report suggested that pretreatment metabolic tumor volume (MTV) on ^{18}F-fluorodeoxyglucose/positron emission tomography can predict the risk of local disease progression in a specific tumor or lymph node after definitive chemoradiation therapy for locally advanced non-small cell lung cancer (NSCLC). The present analysis validates those findings using a separate patient cohort and reports local control probability as a function of pretreatment MTV. These findings may guide future

Background: We previously reported that pretreatment positron emission tomography (PET) identifies lesions at high risk for progression after concurrent chemoradiation therapy (CRT) for locally advanced non-small cell lung cancer (NSCLC). Here we validate those findings and generate tumor control probability (TCP) models.

Methods: We identified patients treated with definitive, concurrent CRT for locally advanced NSCLC who underwent staging ^{18}F-fluorodeoxyglucose/PET/computed tomography. Visible hypermetabolic lesions (primary tumors and lymph nodes) were delineated on each patient's pretreatment PET scan. Posttreatment imaging was reviewed to identify locations of disease progression. Competing risks analyses were performed to examine metabolic tumor volume (MTV) and radiation therapy dose as predictors of local disease progression. TCP modeling was performed to describe the likelihood of local disease control as a function of lesion size.

Results: Eighty-nine patients with 259 hypermetabolic lesions (83 primary tumors and 176 regional lymph nodes) met the inclusion criteria. Twenty-eight patients were included in our previous report, and the remaining 61 constituted our validation cohort. The median follow-up time was 22.7 months for living patients. In 20 patients, the first site of progression was a primary tumor or lymph node treated with radiation therapy. The median time to progression for those patients was 11.5 months. Data from our validation cohort confirmed that lesion MTV predicts local progression, with a 30-month cumulative incidence rate of 23% for lesions above 25 cc compared with 4% for lesions below 25 cc ($P = .008$). We found no evidence that radiation therapy

Reprint requests to: Nitin Ohri, MD, MS, Department of Radiation Oncology, Montefiore Medical Center, Albert Einstein College of Medicine, 111 E 210th St, Bronx, NY 10467. Tel: (718) 920-7750; E-mail: ohri.nitin@gmail.com

Conflict of interest: none.

Int J Radiation Oncol Biol Phys, Vol. 97, No. 2, pp. 372–380, 2017
0360-3016/$ - see front matter
http://dx.doi.org/10.1016/j.ijrobp.2016.10.031

studies of local treatment intensification, deintensification, or both.

dose was associated with local progression risk. TCP modeling yielded predicted 30-month local control rates of 98% for a 1-cc lesion, 94% for a 10-cc lesion, and 74% for a 50-cc lesion.

Conclusion: Pretreatment FDG-PET identifies lesions at risk for progression after CRT for locally advanced NSCLC. Strategies to improve local control should be tested on high-risk lesions, and treatment deintensification for low-risk lesions should be explored.

Introduction

The standard treatment for locally advanced non-small cell lung cancer (NSCLC) for fit patients is a combination of thoracic radiation therapy (RT) with concurrent chemotherapy. ^{18}F-fluorodeoxyglucose positron emission tomography (PET), which is a key component of the staging workup for NSCLC, may also provide important prognostic information for patients treated with (CRT) (1). Locoregional disease progression after CRT may occur in up to 50% of patients (2) despite treatment with RT doses as high as 74 Gy (3).

A previous single-institution retrospective analysis suggested that PET may be used to identify likely sites of locoregional disease progression after CRT (4). Tumors or lymph nodes with a metabolic tumor volume (MTV) exceeding 25 cc had a 2-year cumulative incidence rate for progression of 45%, compared with 5% for smaller lesions. In this report, we analyze a separate cohort of NSCLC patients to validate that finding. We also perform tumor control probability (TCP) modeling, which may guide the development of novel dosing schema for future trials.

Methods

Patient selection

We searched an institutional database for patients treated with definitive concurrent CRT for locally advanced (stage III or unresectable stage II) NSCLC in the years 2007 to 2015 who underwent FDG-PET/CT within 90 days before the start of CRT. Patients treated with induction chemotherapy before CRT or with surgical resection before or after RT were excluded. Data from patients treated between 2011 and 2015 was used to validate previous findings from the 2007 to 2010 cohort. The entire dataset was used for examination of dose-response relationships and TCP modeling.

PET analysis

The PET images were transferred to a commercially available software package (MIMvista Corp, Cleveland, OH). Using a semiautomatic gradient-based contouring algorithm (PET Edge), all visible thoracic hypermetabolic lesions were contoured for each patient by a single observer (N.O.). The lesions were coded as pulmonary tumor or by lymph node station. The MTVs for each lesion were tabulated, as were composite MTVs for each patient.

RT plan analysis

The RT plans were reviewed in our department's treatment planning software (Varian Medical Systems, Palo Alto, CA). Individual gross tumor volumes (GTVs) for each pulmonary tumor and nodal lesion visualized on PET were generated on planning CTs using lung and/or soft tissue window levels, as appropriate. Approximate planning target volumes (PTVs) for each pulmonary, hilar, and mediastinal lesion were generated by expanding each GTV by 10 mm radially and 15 mm in the superior and inferior directions. For apical lung tumors and supraclavicular lymph nodes, expansions of 10 mm in all directions were used. The prescription doses, mean doses, and doses received by 90% of each PTV (D90) were recorded.

Follow-up imaging

We reviewed posttreatment imaging studies for each patient included in this analysis. Imaging with CT or PET/CT was generally performed every 3 months during the first year of follow-up and then every 3 to 6 months afterwards. The incidence and timing of disease progression at each site identified on pretreatment imaging were scored according to the RECIST criteria (5). Biopsy confirmation of progression was rarely obtained.

Statistical analyses: Predictors of local progression

The 2011 to 2015 cohort was used to validate the relationship between MTV and local disease progression previously observed in the 2007 to 2010 cohort. Characteristics of the 2 cohorts were compared by χ^2 testing, the Fisher exact test, unpaired, or Wilcoxon rank-sum test, as appropriate. Lesions from the 2011 to 2015 cohort were grouped by MTV by use of the previously defined cutoff of 25 cc. Cumulative incidence rates of disease progression in each subgroup were calculated.

Table 1 Patient characteristics

Characteristic	2007-2010, n=28	2011-2015, n=61	*P* value	All, n=89
Sex, n (%)			.901*	
Male	16 (57%)	34 (56%)		50 (56%)
Female	12 (43%)	27 (44%)		39 (44%)
Age, mean (range)	62 (49-82)	67 (45-85)	.033	66 (45-85)
Clinical stage, n (%)			.831†	
II	2 (7%)	6 (10%)		8 (9%)
IIIA	21 (75%)	42 (69%)		63 (71%)
IIIB	5 (18%)	13 (21%)		18 (20%)
Interval from PET to RT, median (range)	35 d (0-84)	36 d (6-86)	.561	35 d (0-86)
Total MTV, median (range)	60 cc (10-229)	43 cc (5-404)	.221	51 cc (5-404)
No. of lesions, median (range)	2 (1-12)	3 (1-8)	.634	2 (1-12)
RT dose, median (range)	66.0 Gy (59.4-66)	60.0 Gy (52.5-66.6)	<.001	63.0 Gy (52.5-66.6)
No. of fractions, median (range)	33 (30-37)	25 (25-37)	<.001	30 (25-37)
Chemotherapy regimen, n (%)			<.001†	
Carboplatin/paclitaxel	2 (7%)	53 (87%)		55 (62%)
Cisplatin/etoposide	1 (4%)	6 (10%)		7 (8%)
Cisplatin/pemetrexed	3 (11%)	1 (2%)		4 (4%)
Unknown	22 (79%)	1 (2%)		23 (26%)

Abbreviations: MTV = metabolic tumor volume; PET = positron emission tomography; RT = radiation therapy.
P values obtained with Wilcoxon rank-sum test unless otherwise indicated.
* χ^2 test.
† Fisher exact test.

Disease progression in other treated lesions, disease progression elsewhere, and death of any cause were treated as competing risks. Cumulative incidence rates in the 2 subgroups were compared by the Fine and Gray proportional subhazards model (6). An annotated receiver operating characteristic (ROC) curve was generated to

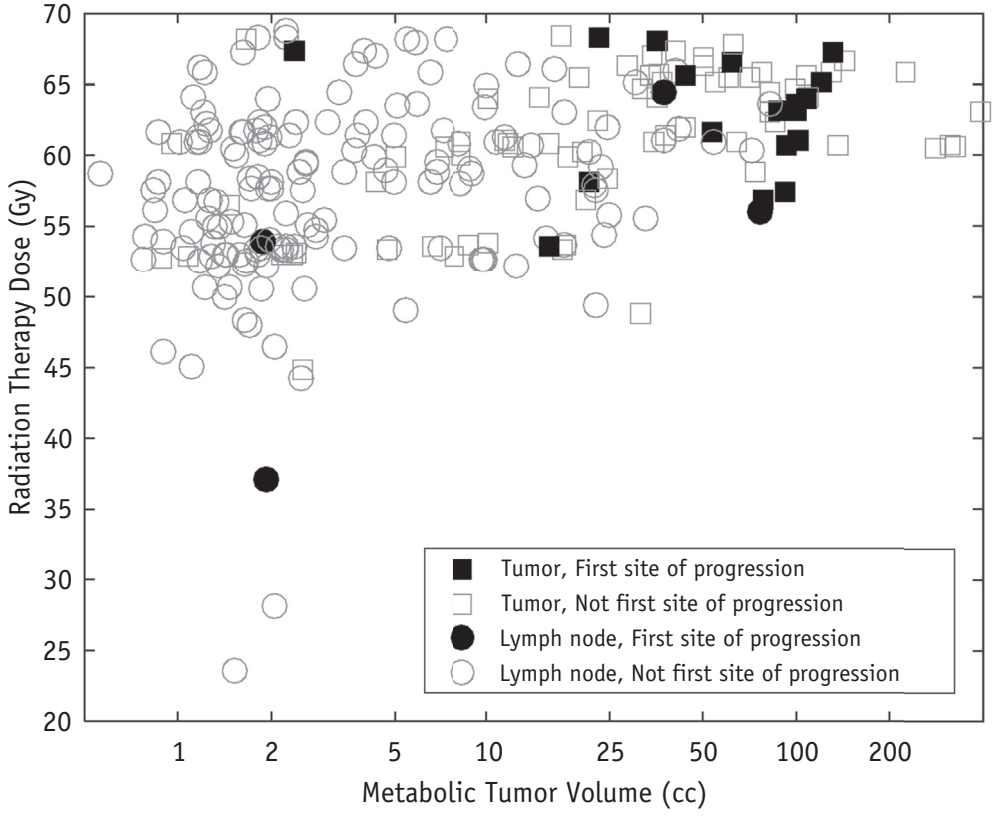

Fig. 1. Scatterplot of radiation therapy dose (PTV D90) versus metabolic tumor volume (MTV). MTV is plotted on a logarithmic scale. Squares represent primary tumors, and circles denote lymph nodes. Lesions that were the first site of disease progression are shaded in black.

depict the utility of MTV for identifying lesions destined to be the first site of disease progression.

We used the Fine and Gray proportional subhazards model to explore associations between RT dose (defined as prescription dose, mean dose, or D90) and local disease progression for the entire dataset and for subgroups of lesions with MTV values below and above 25 cc. Models were run using nominal doses and biologically equivalent doses in 2-Gy fractions (EQD2), calculated by use of the linear quadratic model with $\alpha/\beta = 10$ Gy. We also examined lesion type (tumor vs lymph node) and treatment year as predictors of local progression after adjustment for MTV in multivariable Fine and Gray proportional subhazards models.

On the basis of the results of the analyses described above, we modeled TCP as a function of MTV. In this model, TCP was defined as 1 minus the cumulative incidence rate of local progression 30 months after CRT. The TCP model, where d is the spherical diameter based on MTV, TCD50 is the diameter at which TCP is 50%, and k is a fitting constant that is equal to 25 divided by the slope of the TCP curve at the TCD50, is shown below (7). We used a bootstrap resampling method to characterize the distributions of model parameters and formulate 95% confidence bounds for the TCP curve (8). Lesions were sorted into 4 bins based on diameter for each iteration, and 5000 iterations were performed.

$$TCP = e^{[d-TCD50]/k} \div \left(1 + e^{[d-TCD50]/k}\right)$$

For all analyses, P values $<.05$ were considered statistically significant. All analyses were performed with MATLAB (Mathworks, Natick, MA).

Results

Patient characteristics and clinical outcomes

Eighty-nine patients with 259 hypermetabolic lesions (83 primary tumors and 176 regional lymph nodes) met the inclusion criteria for this analysis. Data from the 61 patients who were treated between 2011 and 2015 were used to validate our findings from the 28 patients treated between 2007 and 2011. The patient characteristics are summarized in Table 1. The median follow-up time was 17.8 months for the entire cohort and 22.7 months for surviving patients.

The MTV for the 259 treated lesions ranged from 0.2 cc to 391.5 cc (median, 4.7 cc; interquartile range, 1.7-23.2 cc). The median RT dose prescribed to each lesion was 60 Gy (range, 52.5-66.6 Gy) over a median course

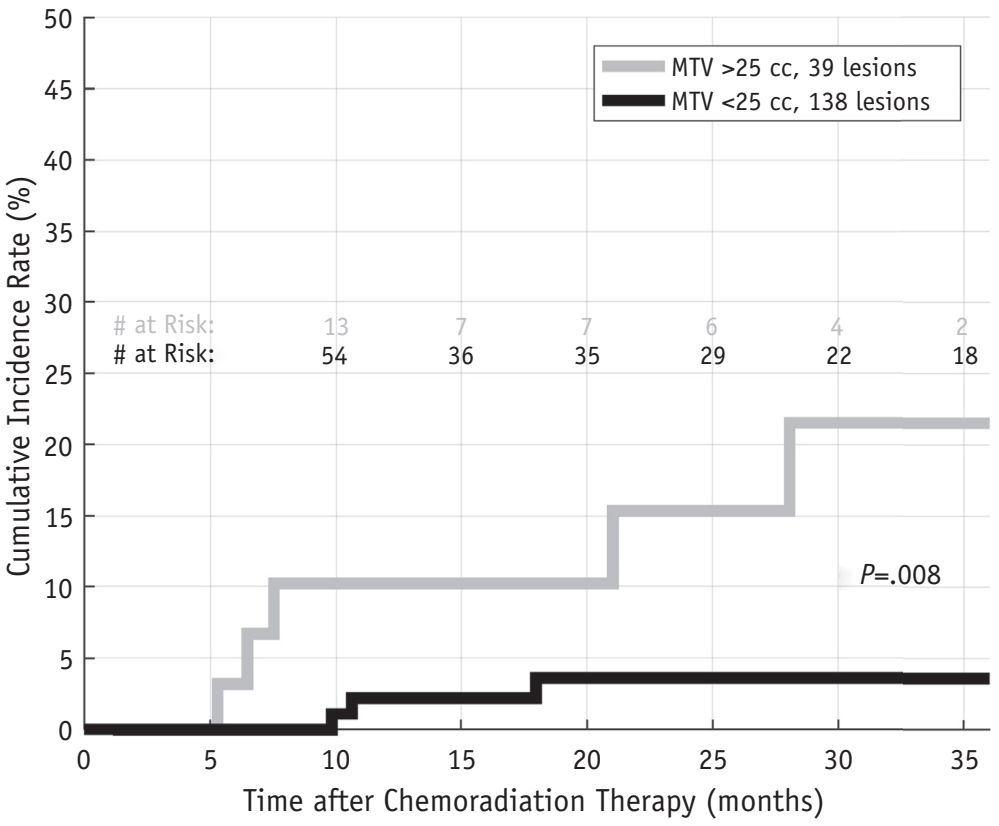

Fig. 2. Cumulative incidence curves for disease progression in tumors or lymph nodes from the validation cohort (61 patients) after grouping by metabolic tumor volume (MTV).

length of 30 fractions (range, 25-37 fractions). Eighty-nine of the 199 lesions with MTV below 25 cc were treated with relatively low prescription doses of 57 Gy (n = 20) or 52.5 Gy (n = 69) as part of an ongoing clinical trial. The median PTV D90 was 60.0 Gy (range, 23.6-68.8 Gy), and the median PTV mean dose was 62.4 Gy (range, 51.7-73.0 Gy). Conversion to EQD2 yielded a median prescription dose of 60.0 Gy_2 (range, 52.9-68.3 Gy_2), a median PTV D90 of 60.0 Gy_2 (range, 21.1-70.8 Gy_2), and a median PTV mean dose of 62.8 Gy_2 (range, 52.0-74.3 Gy_2).

At the time of this analysis, 49 of 89 patients have experienced disease progression. Thirty-two patients have died, 26 of whom experienced disease progression before death. The median progression-free survival time was 12.4 months, and the median overall survival time was 42.5 months.

In 20 of the 49 patients with progressive disease, the first site of progression was a tumor (n = 16) or a lymph node (n = 4) treated with RT. The median time to progression for those patients was 11.5 months (range, 5.3-28.1 months) after the initiation of RT. The median survival time after local progression was 16.7 months.

Predictors of local progression

A scatterplot of RT dose (PTV D90) versus MTV is shown in Figure 1. Cumulative incidence curves for local disease progression in the 2011 to 2015 (validation) cohort after grouping based on the prespecified MTV cutoff of 25 cc are depicted in Figure 2. Cumulative incidence rates of local progression in the validation cohort at 30 months were 23% for lesions with MTV above 25 cc, compared with 4% for lesions with MTV below 25 cc (subdistribution hazard ratio [SHR] = 6.63; 95% CI: 1.63-26.88; $P = .008$). In the entire cohort, 30-month cumulative incidence rates of local progression were 32% for lesions with MTV above 25 cc compared with 5% for lesions with MTV below 25 cc (SHR = 8.29; 95% CI: 3.20-21.50; $P < .001$). Forty-eight of 83 primary tumors had MTVs exceeding 25 cc, and 12 of 176 lymph nodes had MTVs above 25 cc. Exploratory analyses using the entire dataset revealed that a wide range of binary MTV cutoffs could be used to identify lesions at relatively high risk for local disease progression (data not shown), prompting us to perform TCP modeling to better characterize the relationship between MTV and risk of local progression. An annotated ROC curve demonstrating the ability of pretreatment MTV to identify lesions that became the initial site of treatment failure is shown in Figure 3.

Multivariable analysis by the Fine and Gray proportional subhazards model, adjusted for MTV, demonstrated no significant association between RT dose (PTV D90) and risk of local disease progression (SHR = 1.03; 95% CI: 0.91-1.16; $P = .665$). Use of

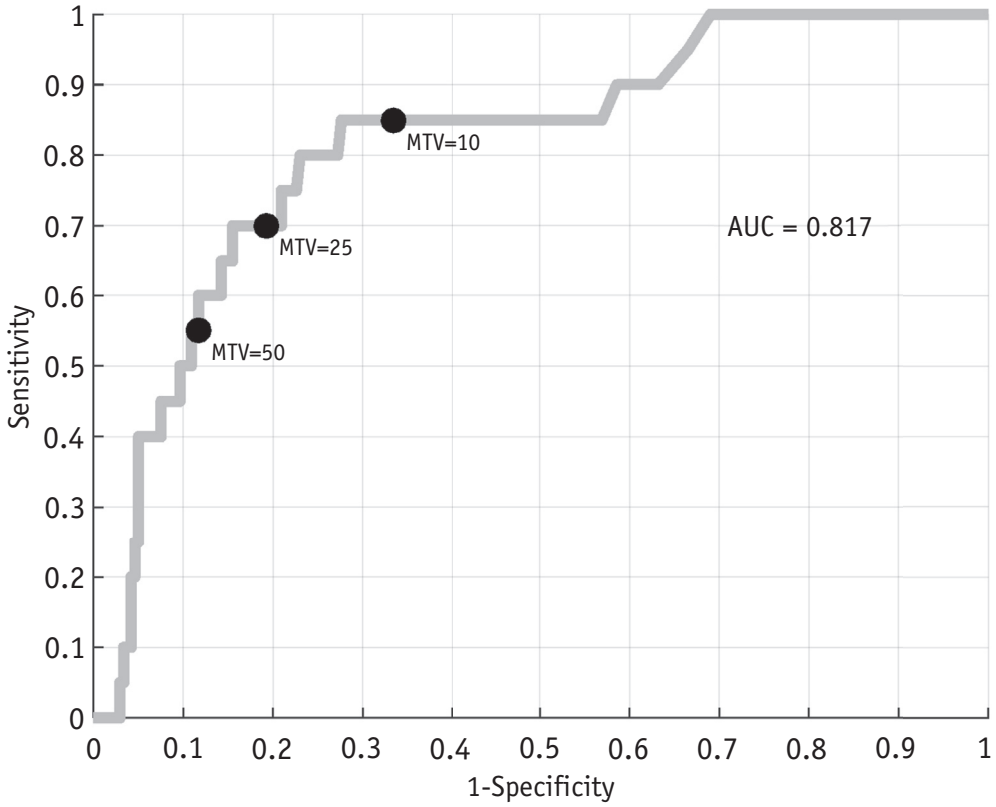

Fig. 3. Receiver operating characteristic curve demonstrating the utility of metabolic tumor volume (MTV) in predicting the initial site of disease progression. *Abbreviation:* AUC = area under the curve.

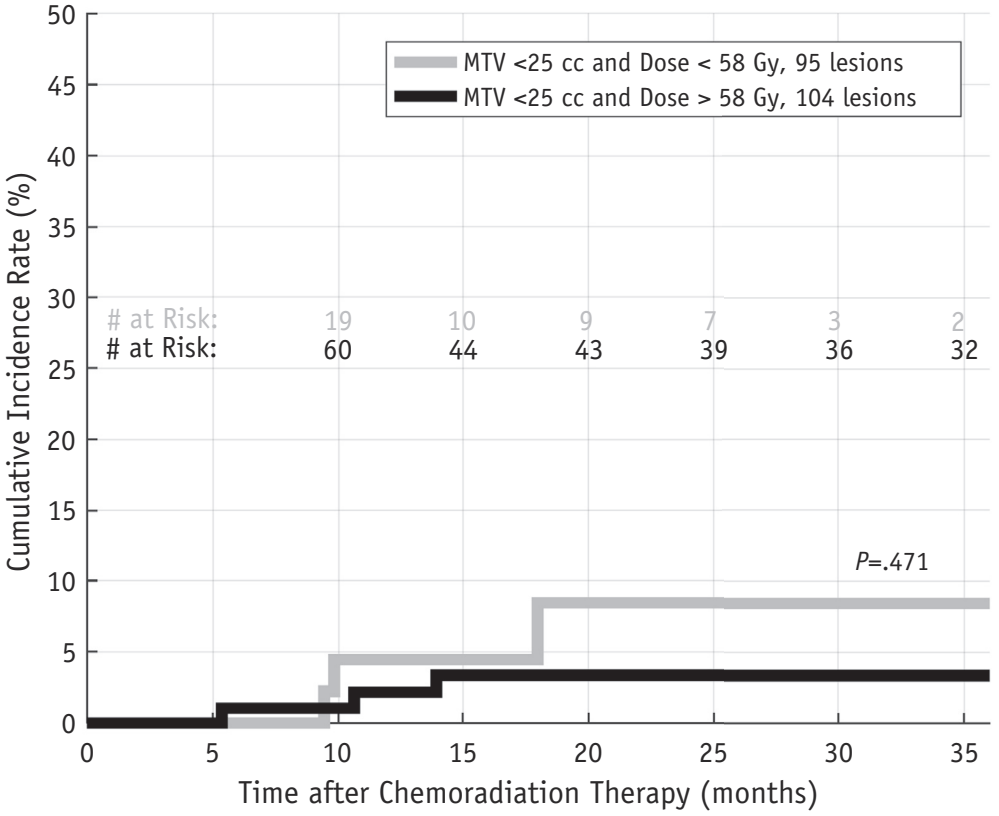

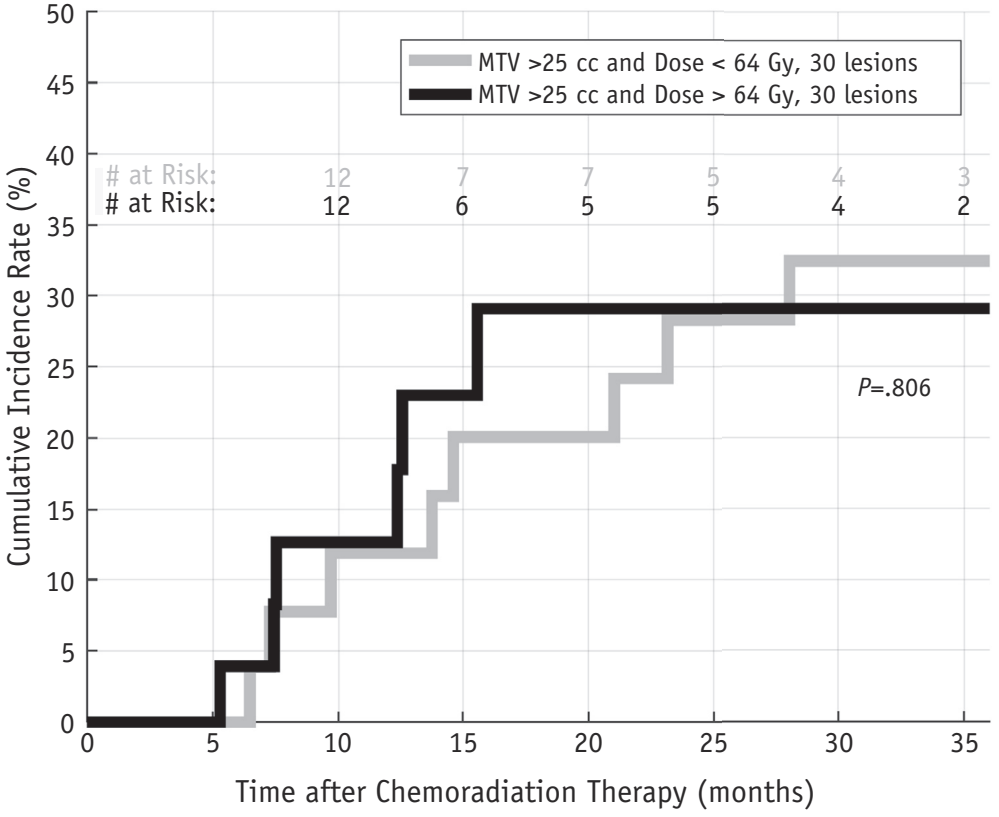

Fig. 4. Cumulative incidence curves for disease progression in tumors or lymph nodes from the entire dataset after grouping by metabolic tumor volume (MTV) and by median radiation therapy dose (PTV D90) for each size cohort.

prescription dose or mean dose in place of PTV D90 similarly did not reveal associations between RT dose and risk of local progression. Conversion of those dose metrics to EQD2 again did not demonstrate any association between RT dose and local progression risk. Cumulative incidence curves for local progression of lesions grouped by MTV and PTV D90 are shown in Figure 4. Multivariable analysis by the Fine and Gray proportional subhazards model, adjusted for MTV, demonstrated no significant association between lesion type and risk of local disease progression (SHR for tumors vs lymph nodes = 2.97; 95% CI: 0.68-12.92; $P = .147$). A multivariable model including treatment date did reveal decreased risk for local progression for treatments delivered in recent years (SHR = 0.81 per year; 95% CI: 0.66-0.99; $P = .039$).

The TCP modeling results are depicted in Figure 5. Bootstrap resampling yielded mean values of −12 for k (SD = 4) and 5.8 cm for TCD50 (SD = 0.8). The negative value for k indicates that TCP decreases as lesion size increases. The R^2 for the model was 0.97. Predicted TCP was 98% (95% CI: 95-100) for a 1-cc lesion, 94% (95% CI: 89-99) for a 10-cc lesion, and 74% (95% CI: 58-84) for a 50-cc lesion.

Discussion

In this analysis, we have validated MTV on pretreatment PET/CT as a predictor of local disease progression in individual tumors or lymph nodes after concurrent CRT for locally advanced NSCLC. We found no evidence that moderately increased RT doses were associated with improved local control. TCP modeling demonstrated that local progression in small lesions is rare, whereas local control of large lesions is often not achieved with conventional CRT.

Our findings may help explain the results of Radiation Therapy Oncology Group 0617, which demonstrated that uniform dose escalation from 60 Gy to 74 Gy does not improve locoregional disease control rates (3). Small tumors and lymph nodes in study participants were likely controlled in both study arms, and control of large lesions was not improved with higher RT dosing. Other studies have also demonstrated that uniform RT intensification does not improve outcomes in locally advanced NSCLC patients receiving concurrent CRT (9). Future trials aiming to improve local treatment for this population should focus on patients or lesions that are unlikely to be controlled with standard therapy.

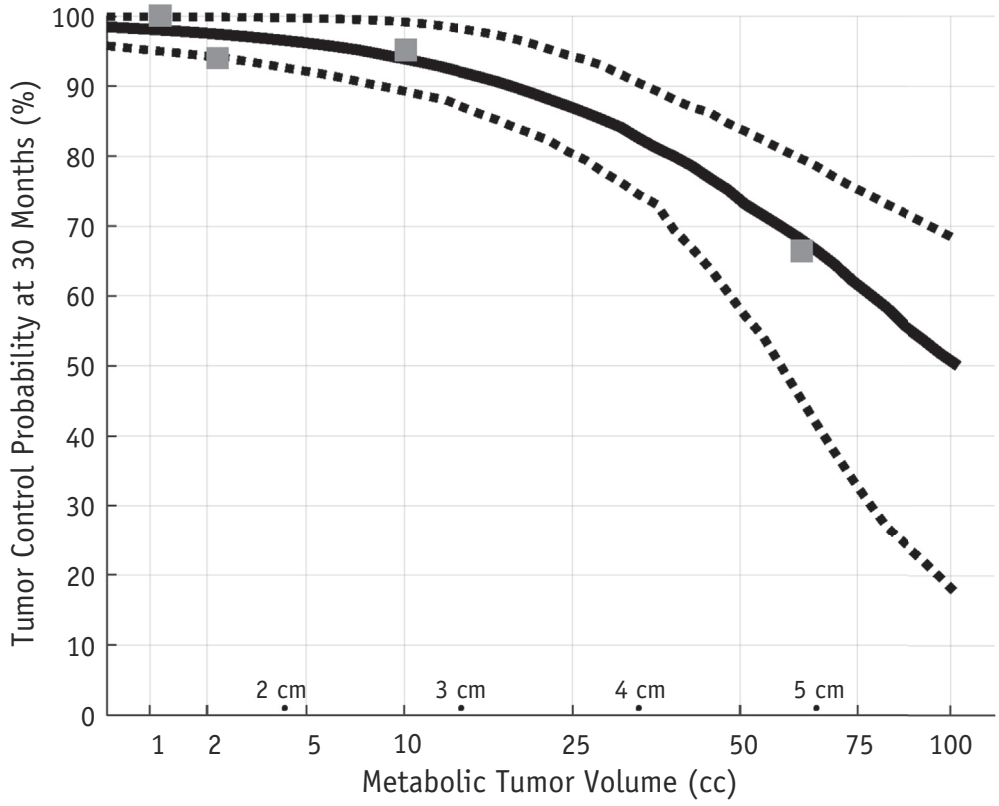

Fig. 5. Tumor control probability (TCP) modeling results. TCP is defined as 1 minus the cumulative incidence rate of local progression 30 months after chemoradiation therapy. Gray boxes represent TCP rates observed in subgroups of 64 to 65 lesions after sorting by size. Five thousand bootstrap iterations were performed. The solid line depicts median TCP, and dotted lines represent 95% confidence results. Selected approximate lesion diameters, calculated assuming spherical geometry, are depicted above the x axis.

Although we successfully validated MTV as a clinically relevant predictor of local control probability after CRT using a binary cutoff of 25 cc, it may be more appropriate to consider MTV as a continuous variable in prediction models. This is supported by our TCP modeling results. Other measures of lesion size such as GTV on CT would also likely predict the risk of local progression (10), but we favor the use of MTV on PET as a prognostic tool because it can quickly be determined using semiautomatic tools that greatly reduce interobserver variability (11).

Interestingly, we found improved local control rates for treatments delivered in recent years. This may be related to advances in treatment planning and delivery that we have implemented over the past 10 years, including use of 4-dimensional CT simulation for treatment planning and daily image guidance for setup verification. More detailed analyses to explore these effects are ongoing.

In addition to measures of disease burden such as MTV defined on PET or GTV defined on CT (12), textural features identified on PET (13) or CT (14) may provide important prognostic information. Further studies are needed to identify features consistently associated with clinical outcomes, and textural features must be evaluated after adjustment for lesion size, which has consistently been shown to be a powerful prognostic factor and is highly correlated with many textural features (15).

Given that dose escalation with conventional RT or slightly hypofractionated RT seems unlikely to improve control rates for large tumors and lymph nodes, other strategies should be explored. A stereotactic body RT boost could be used in many cases, allowing the delivery of higher biologically effective doses and mitigating some concerns about tumor repopulation (16). Multimodality treatment including surgical resection of large primary tumors may also be considered in selected cases (17). Improved systemic therapy may also help prevent progression in lesions treated with RT (18).

In contrast to the disappointing local control rates seen with large lesions, our results indicate that local control rates for lesions with MTV below 10 to 20 cc exceed 90%. Approximately one-third of those lesions were treated with a relatively low prescription dose of 52.5 Gy as part of an ongoing clinical trial, and we found no association between RT dose and local control. This suggests that the current standard dose of 60 Gy may represent overtreatment of many small tumors and regional lymph nodes. Reduction of the RT doses administered to low-risk lesions should be evaluated in prospective trials as a strategy to reduce acute toxicities of CRT (19) and avoid late complications such as cardiac events (20). Reduced RT doses may also be advantageous for combinations of RT and immunotherapy, where pneumonitis may be a major concern (21). Isolated local failures after fractionated RT can often be salvaged with a short course of stereotactic rerirradiation (22).

It is concluded that pretreatment MTV on FDG-PET can be used to identify specific lesions at risk for progression after definitive CRT for locally advanced NSCLC. Strategies to improve local control should be tested on high-risk lesions, and treatment deintensification for low-risk lesions should be explored.

References

1. Ohri N, Duan F, Machtay M, et al. Pretreatment FDG-PET metrics in stage III non−small cell lung cancer: ACRIN 6668/RTOG 0235. *J Natl Cancer Inst* 2015;107.
2. Auperin A, Le Pechoux C, Rolland E, et al. Meta-analysis of concomitant versus sequential radiochemotherapy in locally advanced non-small-cell lung cancer. *J Clin Oncol* 2010;28:2181-2190.
3. Bradley JD, Paulus R, Komaki R, et al. Standard-dose versus high-dose conformal radiotherapy with concurrent and consolidation carboplatin plus paclitaxel with or without cetuximab for patients with stage IIIA or IIIB non-small-cell lung cancer (RTOG 0617): A randomised, two-by-two factorial phase 3 study. *Lancet Oncol* 2015;16:187-199.
4. Ohri N, Piperdi B, Garg MK, et al. Pre-treatment FDG-PET predicts the site of in-field progression following concurrent chemoradiotherapy for stage III non-small cell lung cancer. *Lung Cancer* 2015;87:23-27.
5. Therasse P, Arbuck SG, Eisenhauer EA, et al. New guidelines to evaluate the response to treatment in solid tumors. European Organization for Research and Treatment of Cancer, National Cancer Institute of the United States, National Cancer Institute of Canada. *J Natl Cancer Inst* 2000;92:205-216.
6. Fine JP, Gray RJ. A proportional hazards model for the subdistribution of a competing risk. *J Am Stat Assoc* 1999;94:496-509.
7. Okunieff P, Morgan D, Niemierko A, et al. Radiation dose-response of human tumors. *Int J Radiat Oncol Biol Phys* 1995;32:1227-1237.
8. Deasy JO, Chao KS, Markman J. Uncertainties in model-based outcome predictions for treatment planning. *Int J Radiat Oncol Biol Phys* 2001;51:1389-1399.
9. Yamoah K, Showalter TN, Ohri N. Radiation therapy intensification for solid tumors: A systematic review of randomized trials. *Int J Radiat Oncol Biol Phys* 2015;93:737-745.
10. Werner-Wasik M, Swann RS, Bradley J, et al. Increasing tumor volume is predictive of poor overall and progression-free survival: Secondary analysis of the Radiation Therapy Oncology Group 93-11 phase I-II radiation dose-escalation study in patients with inoperable non-small-cell lung cancer. *Int J Radiat Oncol Biol Phys* 2008;70:385-390.
11. Werner-Wasik M, Nelson AD, Choi W, et al. What is the best way to contour lung tumors on PET scans? Multiobserver validation of a gradient-based method using a NSCLC digital PET phantom. *Int J Radiat Oncol Biol Phys* 2012;82:1164-1171.
12. Bradley JD, Ieumwananonthachai N, Purdy JA, et al. Gross tumor volume, critical prognostic factor in patients treated with three-dimensional conformal radiation therapy for non-small-cell lung carcinoma. *Int J Radiat Oncol Biol Phys* 2002;52:49-57.
13. Tixier F, Hatt M, Valla C, et al. Visual versus quantitative assessment of intratumor 18F-FDG PET uptake heterogeneity: Prognostic value in non-small cell lung cancer. *J Nucl Med* 2014;55:1235-1241.
14. Win T, Miles KA, Janes SM, et al. Tumor heterogeneity and permeability as measured on the CT component of PET/CT predict survival in patients with non−small cell lung cancer. *Clin Cancer Res* 2013;19:3591-3599.
15. Ohri N, Duan F, Snyder BS, et al. Pretreatment 18F-FDG PET textural features in locally advanced non−small cell lung cancer: Secondary analysis of ACRIN 6668/RTOG 0235. *J Nucl Med* 2016;57:842-848.

16. Feddock J, Arnold SM, Shelton BJ, et al. Stereotactic body radiation therapy can be used safely to boost residual disease in locally advanced non-small cell lung cancer: A prospective study. *Int J Radiat Oncol Biol Phys* 2013;85:1325-1331.
17. Albain KS, Swann RS, Rusch VW, et al. Radiotherapy plus chemotherapy with or without surgical resection for stage III non-small-cell lung cancer: A phase III randomised controlled trial. *Lancet* 2009;374:379-386.
18. Herbst RS, Baas P, Kim DW, et al. Pembrolizumab versus docetaxel for previously treated, PD-L1-positive, advanced non-small-cell lung cancer (KEYNOTE-010): A randomised controlled trial. *Lancet* 2016;387:1540-1550.
19. Palma DA, Senan S, Oberije C, et al. Predicting esophagitis after chemoradiation therapy for non-small cell lung cancer: An individual patient data meta-analysis. *Int J Radiat Oncol Biol Phys* 2013;87:690-696.
20. Darby SC, Ewertz M, McGale P, et al. Risk of ischemic heart disease in women after radiotherapy for breast cancer. *N Engl J Med* 2013;368:987-998.
21. Nishino M, Sholl LM, Hatabu H, et al. Anti—PD-1—related pneumonitis during cancer immunotherapy. *N Engl J Med* 2015;373:288-290.
22. Vassil AD, Videtic GM, Stephans KL. Re-irradiation in lung cancer. *J Radiat Oncol* 2015;4:129-139.